Chinese Chemical Letters 34 (2023) 108041

Contents lists available at ScienceDirect

Chinese Chemical Letters

journal homepage: www.elsevier.com/locate/cclet

Enantioselective recognition based on aggregation-induced emission

Pu Chen[a,†], Panpan Lv[a,†], Chang-Sheng Guo[a], Rui-Peng Wang[a], Xiaolong Su[a], Hai-Tao Feng[a,*], Ben Zhong Tang[b,*]

[a] AIE Research Center, Shaanxi Key Laboratory of Phytochemistry, College of Chemistry and Chemical Engineering, Baoji University of Arts and Sciences, Baoji 721013, China

[b] Shenzhen Institute of Aggregate Science and Technology, School of Science and Engineering, The Chinese University of Hong Kong, Shenzhen 518172, China

ARTICLE INFO

Article history:
Received 7 October 2022
Revised 29 November 2022
Accepted 1 December 2022
Available online 5 December 2022

Keywords:
Aggregation-induced emission
Enantioselective recognition
Fluorescent probe
Host-guest interaction
Tetraphenylethylene derivatives
α-Cyanostilbene derivatives
Schiff base derivatives

ABSTRACT

Chirality is one of the most important features of the nature. The recognition of enantiomers plays significant roles in the field of life science, pharmaceutical analysis and food chemistry. Among various recognition methods, fluorescence spectrometry has attracted much attention of researchers thanks to its high sensitivity and easy operation. Compared with traditional fluorescent probes, chiral molecules with aggregation-induced emission (AIE) have drawn increasing interests due to their huge potential in high-efficiency chemo/biosensors and solid emitters. Chiral AIE luminogens (AIEgens) can not only discriminate two enantiomers with excellent enantioselectivity, but also show general applicability for many chiral analytes, such as chiral acids, amino acids, amines, alcohols. In this review, we mainly summarized the recent development of chiral probes with AIE properties, including chiral tetraphenylethylene (TPE) derivatives, α-cyanostilbene derivatives, Schiff base derivatives and other AIEgens. Their synthetic routes, recognition capabilities and possible working mechanisms were well discussed. It is envisioned that the present review can give some significant guidance for design and synthesis of chiral AIEgens with good enantioselectivity and inspire more readers to join the research of chiral AIE.

1. Introduction

Chirality has a crucial role in the research of chemistry [1], pharmacy [2] and biology [3] since many processes cannot proceed smoothly without the participation of chiral compounds. However, enantiomers usually exhibit same physical properties but significant discrepancy in chemical behaviors due to their diverse steric configuration, particularly their biochemical properties [4]. For example, (2*S*,3*R*)-propoxyphene and (2*R*,3*S*)-propoxyphene have been used against pain and cough, respectively [5]. Another striking event was Thalidomide Incident, *R*-thalidomide could relieve nausea and promote sleep in pregnant women, but *S*-thalidomide caused serious phocomelia [6]. Therefore, it is very essential to distinguish different enantiomers to make a clear picture for their individual efficacy. Up to now, several methods have been developed to discriminate a couple of enantiomers, such as HPLC [7], NMR [8], capillary electrophoresis (CE) [9], circular dichroism (CD) [10] and fluorescence spectroscopy [11]. Among them, fluorescence technique has attracted people's attentions due to its low cost, fast response, high sensitivity and selectivity. To now, several reviews have been published that covered a great number of fluorescent sensors for detecting chiral acids, bases and neutral compounds [12,13]. For instance, Pu overviewed a series of chiral fluorescent sensors based on binaphthol (BINOL) derivatives [12]. Yoon summarized different chiral probes based on small organic molecules, metal complexes, polymers and nanomaterials for enantioselective recognition of chiral analytes [13].

Although above-mentioned probes have showed excellent discrimination for enantiomers in organic solvents, it remains a problem that most of them are slightly soluble even insoluble in water. Poor water-solubility of probes may cause aggregation and result in aggregation-caused quenching (ACQ) effect, which limited their further applications [14]. To solve this problem, two major strategies are developed by researchers. The first one is to realize the large dispersion of molecules in the matrix, including doping [15], encapsulating [16] and polymerizing [17], but some additional processes are required. The second method is to develop a new kind of fluorophores to replace these traditional probes. In 2001, a propeller-like organic luminogen was found to be non-emissive in solution but fluoresce strongly in the aggregated state, this fascinating photophysical phenomenon was termed as aggregation-

* Corresponding authors.
E-mail addresses: haitaofeng907@163.com (H.-T. Feng), tangbenz@cuhk.edu.cn (B.Z. Tang).
† These authors contributed equally to this work.

https://doi.org/10.1016/j.cclet.2022.108041
1001-8417/

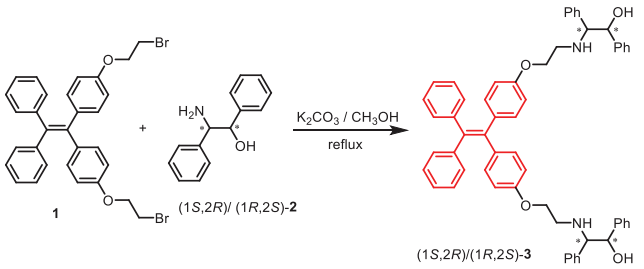

Scheme 1. Synthesis of chiral (1*S*,2*R*)-**3** and (1*R*,2*S*)-**3**.

induced emission (AIE) by Tang for the first time [18]. The popular mechanism for AIE is restriction of the intramolecular motions in the aggregated state, including intramolecular rotations and vibrations [19]. AIE luminogens (AIEgens) effectively overcome ACQ and enriched the variety of fluorescent materials [20–23]. To date, a large number of AIEgens have been developed to apply in the area of theoretical study [24], bioimaging [25] and fluorescence recognition [26] with good performance. Remarkably, AIEgens bearing chiral fragments have served as ideal receptors for discriminating enantiomers thanks to AIE character. Generally, chiral AIEgens can enantioselectively complex with one enantiomer to form aggregates to emit strong fluorescence due to suitable configuration, but the weak interaction with the other enantiomer resulted in faint emission upon complexation. Thus, such differential fluorescence properties can be used to discern two enantiomers by fluorescence technique.

In this review, we mainly discussed ingenious chiral fluorescent probes in enantioselective recognition of chiral acids, amino acids, amines and alcohols based on AIE characteristic for the past few years. Chiral AIEgens were roughly categorized into four kinds according to their different molecular structures, and their synthetic routes, recognition capabilities and possible working mechanisms were presented as well.

2. Chiral recognition by TPE derivatives

Tetraphenylene (TPE), as one of the most popular structural units, was widely existed in AIEgens due to its easy preparation and excellent properties [27]. To date, a series of TPE derivatives have been reported in chiral recognition. In 2012, Zheng's group developed a novel chiral TPE derivative **3** using dibromoethoxy TPE **1** as the starting material (Scheme 1) [28]. As shown in Fig. S1A (Supporting information) and Table 1, (1*S*,2*R*)-**3** could discriminate the enantiomers of chiral diacids **4**, **5**, **6**, **7** and **8** with high enantioselectivity of **25**, **20**, **14**, **20** and **12**, respectively. (1*S*,2*R*)-**3** also exhibited good chiral recognition for monocarboxylic acids and sulfonic acid, such as **9**, **10**, **11**, **12** and **13**, and the enantioselectivity was 5.0, 13, 46, 16 and 5.6, respectively (Table 1).

In addition, the enantioselectivity changed as concentration and solvent(s) were changed. As revealed in Fig. S1B (Supporting information), the enantioselectivity increased quickly with the increasing of concentration in $CHCl_3$. Interestingly, in $CHCl_3$ mixed with *n*-hexane, (1*S*,2*R*)-**3** could recognize the two enantiomers at a very low concentration (10^{-6} mol/L) (Fig. S1C in Supporting information).

The mechanism of aggregates formation was explored using (1*S*,2*R*)-**3** and enantiomers **4** (Fig. 1). ^{1}H NMR titration, Job plots and mass spectra revealed that both D-**4** and L-**4** formed a 1:1 complex with (1*S*,2*R*)-**3**, and corresponding association constants were 6.3×10^4 and 1.3×10^4 L/mol, demonstrating the different binding force during enantiomers with (1*S*,2*R*)-**3**. 2D NOESY spectra indicated that methine protons of acid (H_a) were neared to protons of alkanoic chains (H_d, H_e, H_f and H_g) and the toluoyl group of the acid (H_b) was closed to H_c. The acid **4** approach to amine **3** from exterior of amino group, and the **3-4** complex formed by the acid-base interaction. By the dipole-dipole attraction of two acid-base ion pairs and hydrogen bonds, the tetramer complex **A** was formed. The obtained tetramers constituted a 1D network **B** by further acid-base interaction at the x direction and then the 3D nano-rod was formed by stacking of the **B** side by side at y and z directions. If the 1D network cannot form due to the insufficient interaction force in the tetramer complexes or the insoluble of tetramer, the aggregations will not produce. In aggregates, strong fluorescence will be observed, otherwise, the complexes will emit weak fluorescence.

Amino acids are the basic structural units of biomacromolecules. However, enantioselective recognition of unprotected α-amino acids by a fluorescence method, which is especially challenging due to the zwitterionic property and slight solubility of α-amino acids [29]. To solve this problem, chiral macrocycle compounds (1*S*,2*S*)-**19** and (1*R*,2*R*)-**19** based on TPE were explored by Zheng's group (Scheme 2) [30]. As expected, both of them showed specific AIE properties and good recognition capabilities for α-amino acids.

Table 1
The enantioselectivity (I_1/I_2) of (1*S*,2*R*)-**3** resulted from two enantiomers of chiral acids.

No	Acids	I_1/I_2	State[a]
1	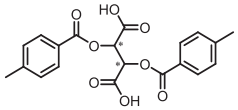 **4**	25 (D/L)	Pre/Sol[b]
2	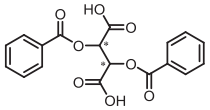 **5**	20 (D/L)	Pre/Sol[b]
3	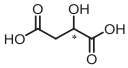 **6**	14 (D/L)	Sus/Sol[c]
4	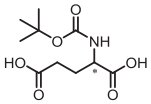 **7**	20 (D/L)	Sus/Sol[c]
5	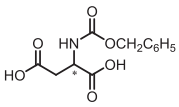 **8**	12 (D/L)	Sus/Sol[c]
6	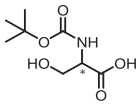 **9**	5 (D/L)	Sus/Sol[d]
7	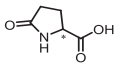 **10**	13 (D/L)	Sus/Sol[c]
8	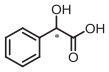 **11**	46 (*R*/*S*)	Sus/Sol[e]
9	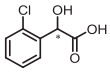 **12**	16 (*R*/*S*)	Sus/Sol[c]
10	 **13**	5.6 (D/L)	Sus/Sol[d]

[a] Enantiomer 1/enantiomer 2, Pre = precipitates, Sus = suspension; Sol = solution. Fluorescence intensity (I) was measured at λ_{max}.
[b] In $CHCl_3$.
[c] In H_2O/THF (tetrahydrofuran).
[d] In CH_2Cl_2.
[e] In CH_2Cl_2/*n*-hexane.

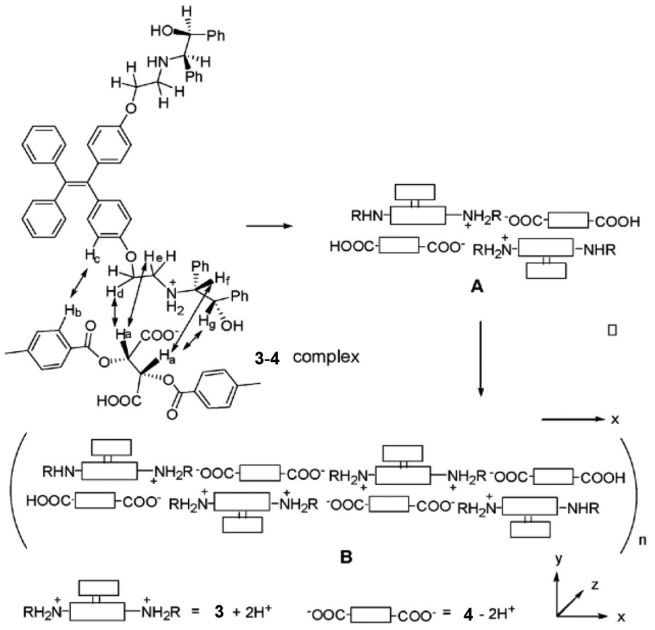

Fig. 1. The main intermolecular NOEs between **3** and **4** in **3**-**4** complexes and probable mechanism of aggregates formation. Copied with permission [28]. Copyright 2012, Royal Society of Chemistry.

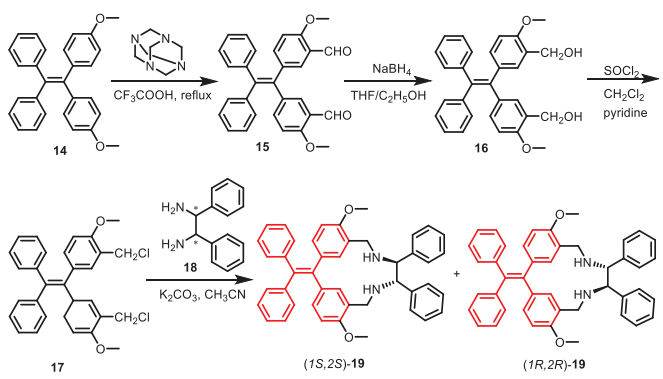

Scheme 2. Synthesis of chiral (1*S*,2*S*)-**19** and (1*R*,2*R*)-**19**.

As shown in Table 2, (1*S*,2*S*)-**19** could discriminate 9 kinds of α-amino acids and four kinds of acids. The mixture of (1*S*,2*S*)-**19** and L-**28** gave a precipitate and emitted strong emission, but the mixture of (1*S*,2*S*)-**19** and D-**28** gave a solution which emitted weak fluorescence, and the selectivity I_L/I_D reached 5.8. ^{1}H NMR titration and 2D NOESY spectra of (1*S*,2*S*)-**19** with enantiomers **11** indicated that *R*-**11** went into the cavity of (1*S*,2*S*)-**19** more deeply than *S*-**11**, which could limit more intramolecular motions and gain stronger emission. This work disclosed that chiral AIE macrocycles played crucial roles in enantioselective recognition.

As a powerful chiral receptor, compound **35** were synthesized by nitration, reduction and nucleophilic reaction (Scheme 3), and could discriminate the enantiomers of chiral acids and bases, and even neutral alcohols [31]. As shown in Table 3, for acids **12**, **11**, **36**, **5** and **4**, amines **38**, **37**, **18** and **34**, α-amino acids **25**, **29**, **26**, **39**, **27** and **28**, alcohols **40**, **41**, **42** and **43**, (*R*,*R*)-**35** could differentiate their enantiomers with enantioselectivity from 2 to 156 in the mixed solvent. The multiple hydrogen bonds and CH-π interactions between the (*R*,*R*)-**35** and the enantiomers played crucial roles in the selective aggregation.

Not only single molecule, the ensembles L-**46** can be also used in chiral recognition [32]. As shown in Scheme 4, L-**46** was obtained by boric acid **44** and L-tartaric acid **45**. In an EtOH/THF so-

Table 2
Enantioselectivity of (1*S*,2*S*)-**19** resulting from two enantiomers of chiral acids.

No	Acids	I_1/I_0[a]	I_1/I_2	State
1	**11**	28.6	8.4	Pre/Sol
2	**13**	26.5	14.6	Pre/Sol
3	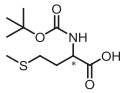 **20**	16.7	4.2	Pre/Sol
4	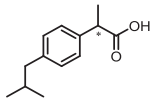 **21**	11.9	2.6	Pre/Sol
5	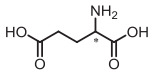 **22**	18.2	1.7	Pre/Sol
6	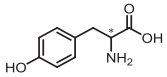 **23**	15.1	2.3	Pre/Sol
7	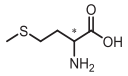 **24**	13.5	2.1	Pre/Sol
8	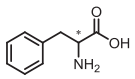 **25**	16.8	2.1	Pre/Sol
9	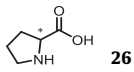 **26**	11.4	2.2	Pre/Sol
10	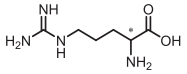 **27**	23.1	1.8	Pre/Sol
11	**10**	10.2	2.4	Pre/Sol
12	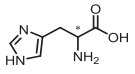 **28**	14.2	5.8	Pre/Sol
13	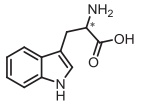 **29**	18.9	2.1	Pre/Sol

[a] I_0 is the intensity of (1*S*,2*S*)-**19** with no acid.

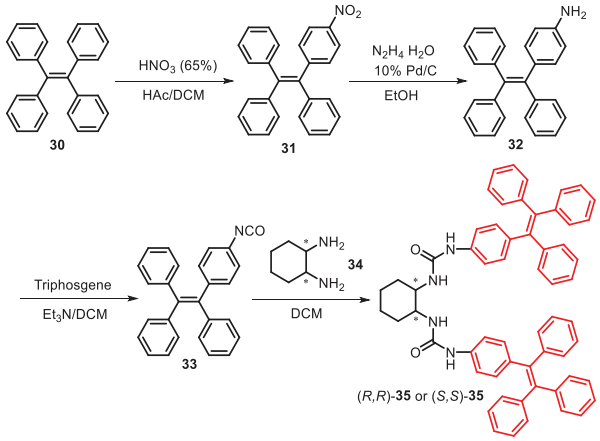

Scheme 3. Synthesis of chiral (*S*,*S*)-**35** and (*R*,*R*)-**35**.

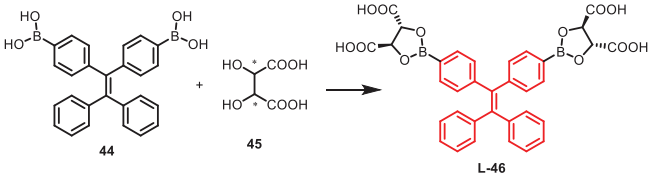

Scheme 4. Synthesis of chiral L-**46**.

Table 3
Fluorescence intensity ratio and state of the mixture of enantiomer of analyte with (*R*,*R*)-**35** in solvent.

No	Analytes	I_1/I_2	State	Mixtures[a]
1	**12**	8.8 (*S*/*R*)	Sus/Sol	7.8×10^{-5} M in *n*-hexane/DCE 3.5:1
2	**11**	5.9 (*S*/*R*)	Sus/Sol	1.0×10^{-4} M in *n*-hexane/DCE 2.7:1
3	 **36**	3.6 (*R*/*S*)	Pre/Sol	8.9×10^{-5} M in *n*-hexane/DCE 4.0:1
4	**5**	3.8 (D/L)	Pre/Sol	8.0×10^{-5} M in *n*-hexane/DCE 5.5:1
5	**4**	9.2 (D/L)	Sus/Sol	8.0×10^{-5} M in *n*-hexane/DCE 4.0:1
6	**13**	63 (L/D)	Pre/Sol	8.5×10^{-5} M in *n*-hexane/DCE 5.9:1
7	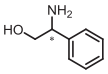 **37**	9.3 (*S*/*R*)	Sus/Sol	7.6×10^{-5} M in *n*-hexane/DCE 4.0:1
8	**18**	2.4 (*SS*/*RR*)	Sus/Sol	7.4×10^{-5} M in *n*-hexane/DCE 3.9:1
9	**34**	33 (*SS*/*RR*)	Sus/Sol	5.4×10^{-5} M in *n*-hexane/DCE 6.0:1
10	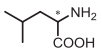 **38**	156 (L/D)	Sus/Sol	1.0×10^{-4} M in H_2O/THF 4.0:1
11	**25**	9.1 (L/D)	Sus/Sol	1.0×10^{-4} M in H_2O/THF 1.6:1
12	**29**	6.2 (L/D)	Sus/Sol	4.5×10^{-5} M in H_2O/THF 1.9:1
13	**26**	2.6 (D/L)	Sus/Sol	1.0×10^{-4} M in H_2O/THF 1.4:1
14	 **39**	3.6 (D/L)	Sus/Sol	1.0×10^{-4} M in H_2O/THF 1.7:1
15	**27**	15.8 (L/D)	Sus/Sol	1.2×10^{-4} M in H_2O/THF 1.6:1
16	**28**	49 (L/D)	Sus/Sol	1.0×10^{-4} M in H_2O/THF 1.5:1
17	 **40**	2.5 (L/D)	Sus/Sol	1.3×10^{-4} M in H_2O/THF 1.7:1
18	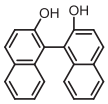 **41**	2.0 (*R*/*S*)	Sus/Sol	1.2×10^{-4} M in H_2O/THF 1.9:1
19	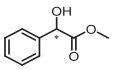 **42**	55 (*S*/*R*)	Sus/Sol	5.8×10^{-5} M in *n*-hexane/DCE 3.6:1
20	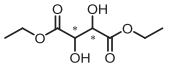 **43**	3.3 (L/D)	Sus/Sol	8.1×10^{-5} M in *n*-hexane/DCE 4.0:1

[a] Volume ratio of solvents. DCE = 1,2-dichloroethane. [(*R*,*R*)-**35**] = [analyte]. M = mol/L.

Table 4
Fluorescence intensity ratio and state of the mixture of enantiomer of analyte with L-**46** in solvent.

No	Acids	I_1/I_2	Mixtures[a]
1	**34**	8.48 (*SS*/*RR*)	1.5 mM in EtOH/THF 4:1
2	**18**	0.391 (*SS*/*RR*)	1.5 mM in EtOH/THF 1:5
3	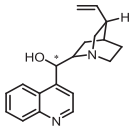 **47**	-[b]	1.0 mM in THF

[a] mM = mmol/L.
[b] not clear.

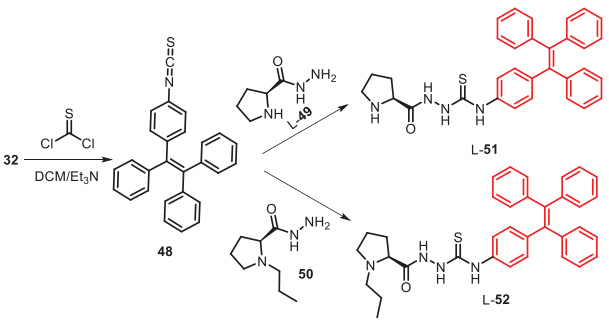

Scheme 5. Synthesis of compounds L-**51** and L-**52**.

lution, the mixture of L-**46** and (1*S*,2*S*)-**34** emitted bright blue fluorescence, while the mixture of L-**46** and (1*R*,2*R*)-**34** showed weak emission (Table 4 and Fig. S2A in Supporting information). In addition, L-**46** also could discriminate the enantiomers of **18** and natural alkaloids **47** (Table 4 and Figs. S2B and C in Supporting information).

Chiral fluorescent probes L-**51** and L-**52** could be gained in two steps by amine **32** (Scheme 5). However, L-**51** could be used in chiral recognition of unprotected amino acids, acids, amines and alcohols [33]. For amino acids, the mixture of D-**53**, D-**26** or D-**25** and L-**51** induced suspension, but the mixture of L-**53**, L-**26** or L-**25** still

Table 5
Fluorescence intensity ratio and state of the mixture of enantiomer of analytes with L-**51** in mixed solvents. [L-**51**] = [analyte].

No	Analytes	I_1/I_2	State	Mixtures[a]
1	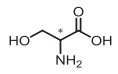 **53**	1.9 (D/L)	Sus/Sol	2.8×10^{-4} M in THF/H_2O 1:2.6
2	**26**	4.6 (D/L)	Sus/Sol	3.6×10^{-4} M in THF/H_2O 1:1.8
3	**25**	4.5 (D/L)	Sus/Sol	2.9×10^{-4} M in THF/H_2O 4.0:1
4	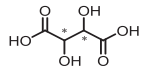 **54**	2.6 (D/L)	Sus/Sol	3.6×10^{-4} M in THF/H_2O 1:1.8
5	**41**	3.3 (*S*/*R*)	Sus/Sol	3.7×10^{-4} M in THF/H_2O 1:1.7
6	**43**	2.8 (D/L)	Sus/Sol	4.2×10^{-4} M in THF/H_2O 1:1.4
7	**42**	5.8 (*S*/*R*)	Sus/Sol	3.9×10^{-4} M in THF/H_2O 1:1.6
8	**37**	2.9 (*S*/*R*)	Sus/Sol	3.9×10^{-4} M in THF/H_2O 1:1.6
9	 **55**	5 (*R*/*S*)	Sus/Sol	3×10^{-4} M in THF/H_2O 1:2.3
10	**34**	1.8 (*RR*/*SS*)	Sus/Sol	2.8×10^{-4} M in THF/H_2O 1:2.6

[a] M = mol/L.

remained a clear solution in the mixed solvents of THF and H_2O, and the enantioselectivities were 1.9, 4.6 and 4.5, respectively. For acid **54**, alcohols **41**-**43**, amines **34**, **37** and **55**, L-**51** could distinguish their enantiomers with enantioselectivity from 1.8 to 5.8 in the THF/H_2O (Table 5). But L-**52** showed poor selectivity in chiral recognition, this comparison indicated that hydrogen bonds between L-**51** and enantiomers play key roles in chiral recognition.

Remarkably, most chiral recognitions were based on fluorescence intensity changes of fluorescent probe and two enantiomers. Only very limited works on the chiral recognition based on emission wavelength change. In 2020, Zheng's group designed and synthesized chiral fluorescent probe *S*-**62** that could discriminate enantiomers and give different colors [34]. *S*-**62** was directly synthesized using compound **56** as the starting material (Scheme 6).

As depicted in Fig. 2B, *S*-**62** emitted yellow light in the mixed solvent of cyclohexane/acetone. After D-**4** was mixed in *S*-**62**, the emission of the mixture was changed from yellow to blue, while the mixture of *S*-**62** with L-**4** emitted green light, both D-**4** and L-**4** could enhance the intensity of *S*-**62** and showed a very small intensity difference. In addition, chiral dicarboxylic acids including **63**, **5**, **54**, **64**, **65**, **6** and **66**, monocarboxylic acids such as **42**, **12**, **10**, **67** and **68** also showed different colors between their enantiomers when they mixed with *S*-**62** (Fig. 2C). The crystal structure of *S*-**62**-*S*-**12** complex revealed that the carboxylate anion was inserted between two phenyl rings of TPE and forming strong hydrogen bonds with two ammonium group of *S*-**62**. The phenyl rings rotated toward the direction vertical to the double bond, which resulted the decreasing conjugation and hypochromic shift. Adding different enantiomer induced the disparate degree of phenyl ring rotation, which result in different color changes.

In 2021, a pair of chiral AIEgens *R*-**72** and *S*-**72** were synthesized by our group using **69** as a start material (Scheme 7) [35]. In the mixed solvents of *n*-hexane and THF, *R*-**72** could recognize the two enantiomers of **21** and **4** with high selectivity of 12.6 and 5.9 (Figs. S3A and B in Supporting information), respectively. Besides the above acids, *R*-**72** is also suitable for discriminating of camphorsulfonic acid **13** ($I_R/I_S = 2.4$), cysteine **73** ($I_D/I_L = 6.5$), Boc-

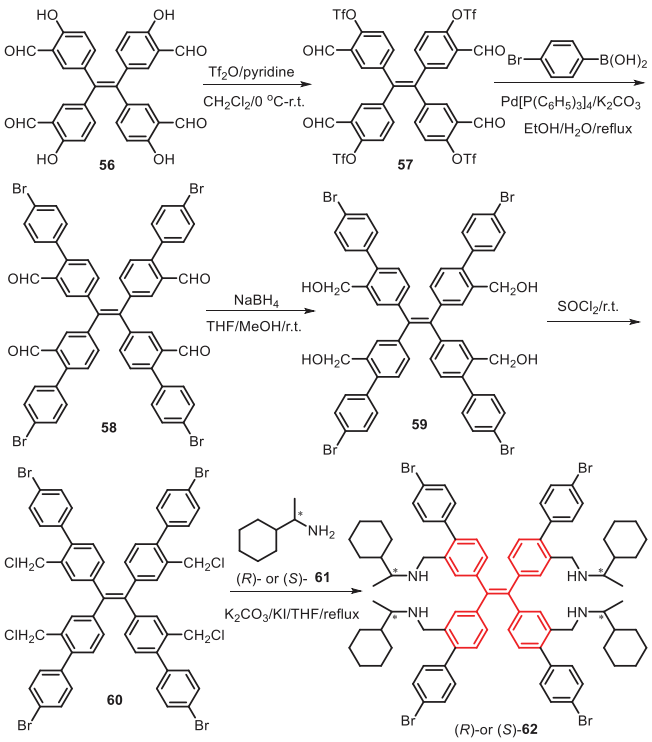

Scheme 6. Synthesis of (*R*)-or (*S*)-**62**.

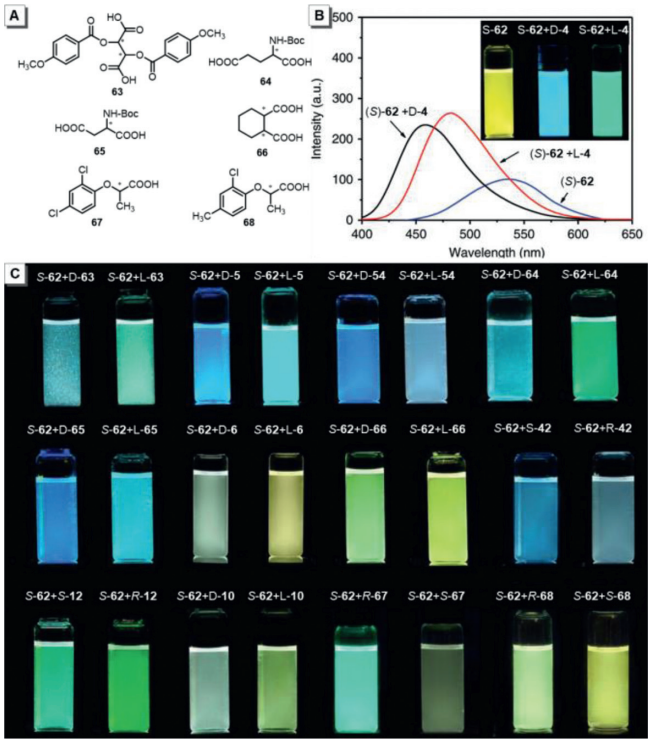

Fig. 2. (A) Chemical structures of chiral carboxylic acids, (B) Emission spectra of (*S*)-**62** after mixing with two enantiomers of **4** (**4**/(*S*)-**62** = 2:1, molar ratio) in cyclohexane/acetone 98:2. Insets and (C) photos of solution of (*S*)-**62** without and with chiral acid enantiomers under 365 nm light. Copied with permission [34]. Copyright 2020, Nature.

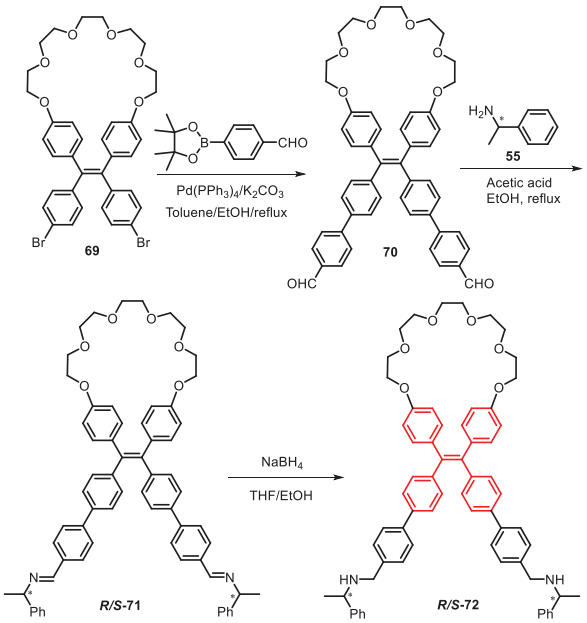

Scheme 7. Synthesis of (*R*)-and (*S*)-**72**.

phenylalanine **74** ($I_D/I_L = 2.4$) and Boc-serine **9** ($I_L/I_D = 2.0$) (Table 6).

Unfortunately, *R*-**72** cannot efficiently discriminate enantiomers **54** or **76** (Figs. S3C and E in Supporting information). Considering the important applications of host-guest interaction, a supramolecular assembly strategy was used in chiral recognition. As depicted in Figs. S3D and F (Supporting information), assembled mixture of *p*-sulfonatocalix[4]arene **75** and *R*-**72** showed high enantioselectivity for tartaric acid **54** with high fluorescence intensity ratio of 2.9 (Fig. S3D). Similarly, enantiomers **76** could be recognized with an enantioselectivity of 3.1 (Fig. S3F).

Very recently, two TPE-based chiral AIEgens *R*-**80** and *S*-**80** bearing two L-cyclohexylethylamine were synthesized (Scheme 8) by our group [36]. As shown in Figs. 3A and B, *R*-**80** could interact with D-**7** to afford a gel in DCE with strong fluorescence, while the mixture of *R*-**80** and L-**7** still maintained a solution without obvious emission, and the enantioselectivity is up to 103. The microstructure of *R*-**80** and D-**7** generated numerous nanospheres, and formed a string of necklace-like clusters (Fig. 3C).

Table 6
Fluorescence intensity ratio and state of the mixture of enantiomer of analytes with *R*-**72** in mixed solvents.

No	Acids	I_1/I_2	State	Mixtures[a]
1	**21**	12.6 (*R*/*S*)	Sus/Sol	8.0×10^{-6} M in *n*-hexane/THF 7:3
2	**4**	5.9 (L/D)	Sus/Pre	5×10^{-5} M in *n*-hexane/THF 7:3
3	**13**	2.4 (*R*/*S*)	-	8.3×10^{-6} M in THF/*n*-hexane 1:9
4	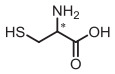 **74**	6.5 (D/L)	-	8.3×10^{-6} M in THF/*n*-hexane 1:9
5	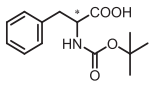 **75**	2.4 (D/L)	-	1.67×10^{-5} M in THF/*n*-hexane 1:9
6	**9**	2.0 (L/D)	-	8.3×10^{-6} M in THF/*n*-hexane 1:9

[a] M = mol/L.

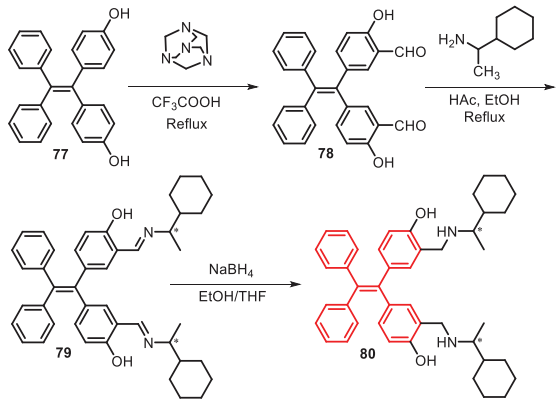

Scheme 8. Synthesis procedure of (*R*)-and (*S*)-**80**.

Strong fluorescence was observed due to its AIE effect. Correspondingly, the mixture of *R*-**80** and L-**7** afforded a clear solution, and chrysanthemum-like structures were gained after solvent evaporation.

As depicted in Figs. 3E and F, *R*-**80** showed excellent discrimination for di-*p*-toluoyl-tartaric acid **4**. And other chiral acids and unprotected amino acids, listed in Table 7, could also be discrimi-

Table 7
Fluorescence intensity ratio and state of the mixture of *R*-**80** and chiral acids, [*R*-**80**] = [analyte].

No	Acids	I_1/I_2	State	Mixtures[a]
1	**7**	103 (D/L)	Gel/Sol	1×10^{-3} M in DCE
2	**12**	2.5 (*S*/*R*)	Pre/Sol	3.75×10^{-4} M in DCE/*n*-hexane 3:1
3	**9**	4.2 (L/D)	Pre/Sol	5×10^{-4} M in DCE
	5	6.4 (D/L)	Pre/Sol	5×10^{-4} M in DCE
5	**4**	4.5 (D/L)	Sus/Pre	3×10^{-4} M in DCE/*n*-hexane 3:2
6	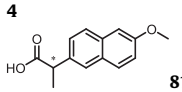 **81**	3 (*S*/*R*)	Pre/Sol	2.38×10^{-5} M in DCE/*n*-hexane 1:20
7	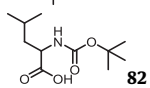 **82**	3.8 (D/L)	Pre/Sol	5×10^{-4} M in DCE
8	**13**	20 (D/L)	Pre/Sol	1.43×10^{-4} M in DCE/*n*-hexane 2:5
9	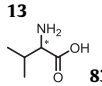 **83**	3 (L/D)	Pre/Sol	5×10^{-4} M in DMSO
10	**26**	4.4 (D/L)	Pre/Sol	5×10^{-4} M in DMSO
11	**24**	2.5 (D/L)	Pre/Sol	5×10^{-4} M in DMSO
12	**23**	26 (L/D)	Pre/Sol	1×10^{-3} M in DCE

[a] DMSO, dimethylsulfoxide. M = mol/L.

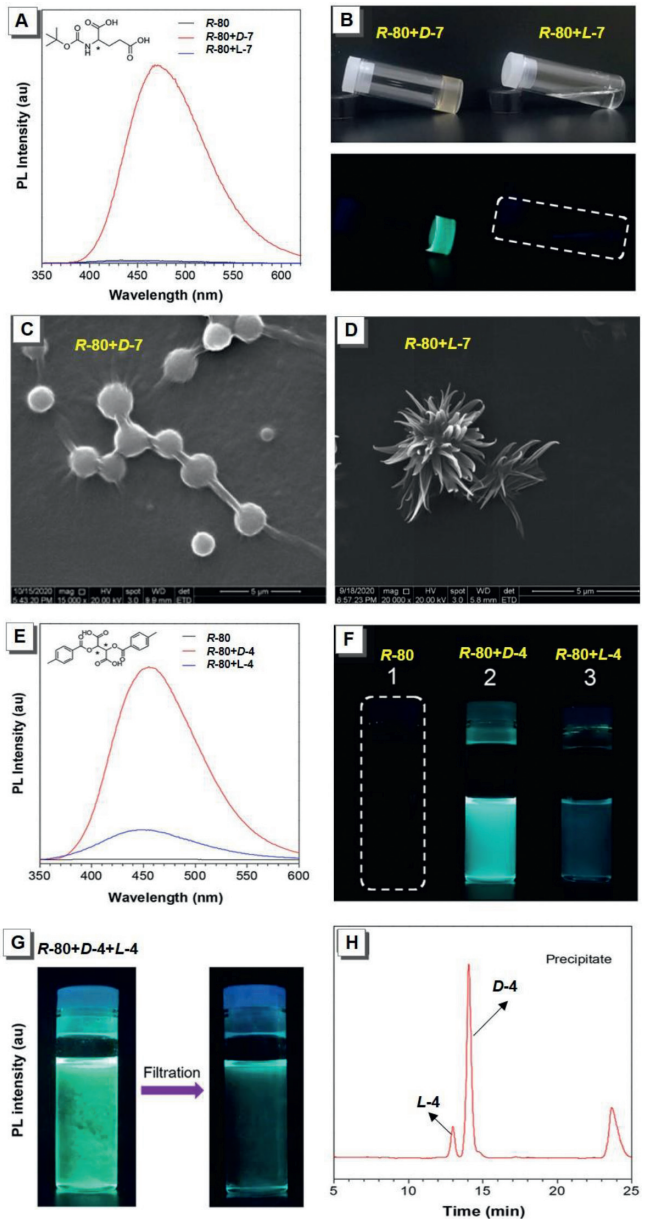

Fig. 3. (A) PL spectra of *R*-**80** and their mixtures of *R*-**80** and D/L-**7** in DCE. (B) Photos of a gel formed in the mixture of *R*-**80** and D-**7** and a solution formed in the mixture of *R*-**80** and L-**7** in DCE under daylight (top) and a portable 365 nm UV lamp (bottom). SEM images of the solution generated by (C) *R*-**80** and D-**7**, (D) *R*-**80** and L-**7** in DCE. (E) PL spectra of *R*-**80** and their mixtures of *R*-**80** and D/L-**4** in DCE. (F) Fluorescent photos of *R*-**80** (1), a suspension of *R*-**80** and D-**4** (2), and a solution of *R*-**80** and L-**4** (3) in DCE. (G) Fluorescent photos of enantioselective separation of D-**4** in the mixture of D-**4** and L-**4** using *R*-**80**. (H) Chiral HPLC results of the precipitates were analyzed on the chiral-phase column of CHIRALPAK IE. Copied with permission [36]. Copyright 2022, American Chemical Society.

nated by *R*-**80** in single or mixed solvent. According to mechanism study, ionic compounds were easily formed by the amino group of *R*-**80** and carboxyl groups of D-**7** due to the acid-base interaction. Hydrogen bonds between *R*-**80** and D-**7** also played important roles in restricted free rotation of phenyl rings of TPE and caused enhanced emission. More importantly, *R*-**80** or *S*-**80** could be used in measuring the optical purity and separating the mixture of chiral acid. As shown in Fig. 3G, adding the mixture of D-**4** and L-**4** in the solution of *R*-**80**, and stored for 30 min. A turbid solution with an intense fluorescence was obtained. Because of the applicable assemblage, the filterable precipitates exhibited high enantioselectivity (Fig. 3H).

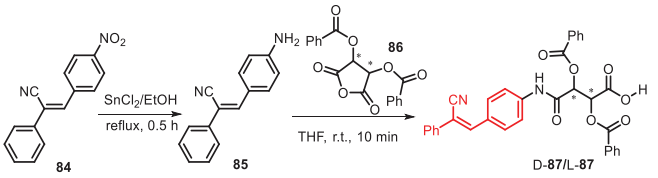

Scheme 9. Synthesis of chiral AIE compounds D-**87** and L-**87**.

Table 8
Interaction results of L-**87** with chiral amines in solvents.[a]

Amine	State	Amine	State
(1*S*,2*R*)-**88**	Solution	(1*R*,2*R*)-**18**	Suspension[b]
(1*R*,2*S*)-**88**	Precipitates	(1*S*,2*S*)-**18**	Solution[b]
R-**37**	Solution	*R*-**17**	Precipitates
S-**37**	Suspension	*S*-**17**	Solution

[a] 0.02 mol/L L-**87** and 0.02 mol/L amine in DCE at approximately 5 °C.
[b] 0.01 mol/L L-**87** and 0.01 mol/L amine in mixed solvent of *n*-hexane and DCE (3:2, v/v).

3. Chiral recognition by α-cyanostilbene derivatives

α-Cyanostilbene derivatives is one of typical AIE compounds [37]. In 2009, Zheng's group synthesized chiral D-**87** and L-**87** by 4-amino-α-cyanostilbene **85** and debezoyltartaric anhydride **86** in excellent yield (Scheme 9) [38]. As revealed in Table 8, aggregates formed selectively when L-**87** mixed with (1*R*,2*S*)-**88**, *S*-**37**, (1*R*,2*R*)-**18** or *R*-**17** in DCE or mixed solvent. In aqueous ethanol, L-**87** could discriminate the enantiomers of **88**, **37**, **18** and **55** with high enantioselectivity of 262, 10, 18 and 17, respectively. Correspondingly, when D-**87** was mixed with (1*S*,2*R*)-**88**, *R*-**37** or (1*S*,2*S*)-**18**, suspensions were more easily formed and showed strong fluorescence. In addition, the chiral excess could be determined by changes in fluorescence.

The morphologies of the aggregates were also investigated by FE-SEM (field emission scanning electron microscopy) [39]. As shown in Fig. 4C, many nanofibers were produced after adding (1*S*,2*R*)-**88** to the solution of D-**87**. The mixture of D-**87** and (1*R*,2*S*)-**88** were composed of round nanospheres (Fig. 4D). The morphologies of D-**87**, D-**89** and D-**90** mixed with enantiomers of amines were summarized in Table S1 (Supporting information). When water was slowly added into the stirring THF solution of D-**87**, D-**89**, D-**90**, D-**91** or D-**92** with enantiomers, such as **88**, **18** and **37**, the aggregates were nanospheres with a hole. The single-hole nanospheres were more easily formed by the mixture of D-**93** and chiral amines due to the long-chain of D-**93**, and the size of the holes was increased with the addition of the water (Figs. 4E-H). The compounds **87**, **89**, **90**, **91**, **92** and **93** were wedge shaped, after combining with amines **88**, **11** or **37**, the acquired complexes were also wedge shaped, then planar and conjugated complex might arrange in parallel and result in nanofibers **E**, while twisted complex might form a circular arrangement and lead to nanosphere **H** (Fig. 4I).

Chiral amines (1*R*,2*S*)-**95** and (1*S*,2*R*)-**95** were able to discriminate the enantiomers of chiral carboxylic acid **5** and **11** with very high fluorescence intensity ratio [40]. As shown in Scheme 10, compound **85** reacted with chloroacetylchloride to give **94**, which was easily attached by a chiral amine to obtain chiral AIE compound **95**. Interaction of (1*S*,2*R*)-**95** and D-**5** or *S*-**11** led to a suspension, while the mixture of (1*S*,2*R*)-**95** and L-**5** or *R*-**11** remained a clear solution, and the enantioselectivity were 196 ($I_{D\text{-}5}/I_{L\text{-}5}$) and 598 ($I_{S\text{-}11}/I_{R\text{-}11}$), respectively. Correspondingly, (1*R*,2*S*)-**95** could dif-

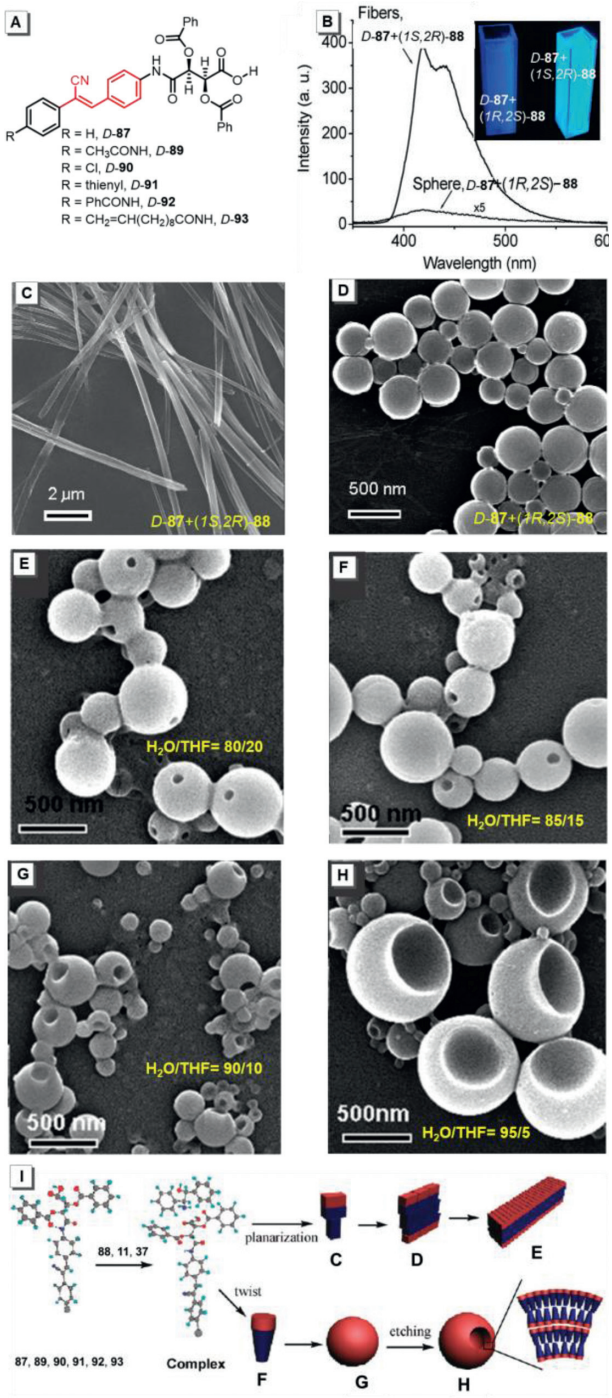

Fig. 4. (A) Structures of D-**87**, **89**-**93**; (B) PL spectra of D-**87** interacted with enantiomers of **88**; SEM image of mixture of (C) D-**87** and (1*S*,2*R*)-**88**, (D) D-**87** and (1*R*,2*S*)-**88**, [**88**] = [**87**] = 1.0×10^{-3} mol/L in water/ethanol (9:1, v/v). FE-SEM images of suspension of D-**93** and (1*R*,2*R*)-**18** in water/THF, v/v (E) 80:20; (F) 85:15; (G) 90:10 under no stirring ([D-**93**] = [(1*R*,2*R*)-**18**] = 1.0×10^{-3} mol/L). (H) Suspension of D-**93** and (1*R*,2*R*)-**18** in H_2O/THF by evaporating THF 1:1 to 95:5 (v/v). (I) Schematic illustration for the formation of nanofibers, nanospheres, and hollow nanospheres with a hole. Copied with permission [39]. Copyright 2011, American Chemical Society.

ferentiate the enantiomers of **5** and **11** in 1,2-DCE and exhibited high enantioselectivity of 506 ($I_{L\text{-}5}/I_{D\text{-}5}$) and 160 ($I_{R\text{-}11}/I_{S\text{-}11}$), respectively.

As shown in Scheme 11, chiral α-cyanostilbene derivative (*R*,*R*)-**98** was synthesized from compound **96** and **97** in two steps, (*R*,*R*)-**98** showed not only exceptionally high enantioselectivity but also

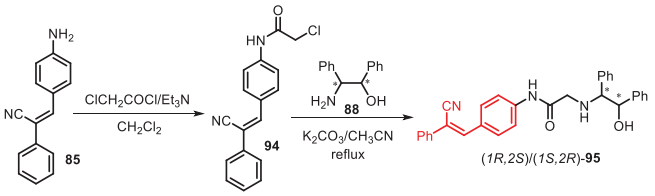

Scheme 10. Synthesis of chiral AIE compounds (1*R*,2*S*)/(1*S*,2*R*)-**95**.

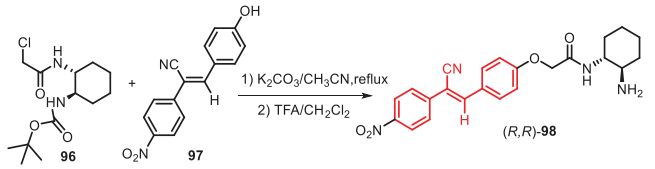

Scheme 11. Synthesis of compound (*R*,*R*)-**98**.

Table 9
Fluorescence intensity ratio and state of the two carboxylic acid enantiomers with (*R*,*R*)-**98** in solvent(s).

No	Acids	I_1/I_2	State
1	**11**	16865 (*S*/*R*)	Pre/Sol
2	**12**	261 (*R*/*S*)	Pre/Sol
3	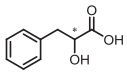 **99**	1000 (*S*/*R*)	Sus/Sol
4	**81**	26 (*S*/*R*)	Sus/Sol
5	**21**	30 (*S*/*R*)	Sticky/Sol
6	**76**	410 (*S*/*R*)	Sus/Sol
7	**10**	410 (*S*/*R*)	Sus/Sol
8	**5**	249 (*RR*/*SS*)	Sus/Sol
9	**4**	2240 (*RR*/*SS*)	Sus/Sol
10	**6**	769 (*S*/*R*)	Sus/Sol
11	**7**	117 (*S*/*R*)	Sus/Sol
12	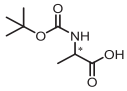 **100**	55 (*S*/*R*)	Sus/Sol
13	**74**	10 (*S*/*R*)	Sus/Sol
14	**9**	59 (*S*/*R*)	Sus/Sol
15	**20**	18 (*R*/*S*)	Pre/Sol
16	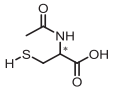 **101**	1717 (*S*/*R*)	Pre/Sol
17	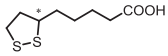 **102**	287 (*S*/*R*)	Sus/Sol
18	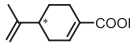 **103**	59 (*S*/*R*)	Gel/Sol

could be used to a wide variety of chiral carboxylic acids [41]. For α-hydroxycarboxylic acids **11**, **12** and **99**, the aggregates formed from a mixture of *S*-**11**, *R*-**12** or *S*-**99** with (*R*,*R*)-**98**, but the mixture of *R*-**11**, *S*-**12** or *S*-**99** with (*R*,*R*)-**98** still remained in solution, and the fluorescence intensity ratio of two enantiomers of **11**, **12** and **99** were 16865, 261 and 1000, respectively (Figs. S4A and B in Supporting information, Table 9). For other carboxylic acids, such as **81**, **21**, **76**, **10**, **5**, **4**, **6**, **7**, **100**, **74**, **9**, **20**, **101**, **102** and **103**, (*R*,*R*)-**98** could also discriminate their enantiomers with excellent enantioselectivity (Table 9). The selective interaction of (*R*,*R*)-**98** with the enantiomers of acids were investigated. As shown in Figs. S4C and D (Supporting information), H_j was closed to H_e in the mixture of (*R*,*R*)-**98** and *S*-**11**. But in the mixture of (*R*,*R*)-**98** and *R*-**11**, H_g was remoted from the H_e. Due to the inward proton and outward hydroxyl group, aggregates were more easily formed though hydrogen bonds and increased polarity between (*R*,*R*)-**98**-*S*-**11** complexes.

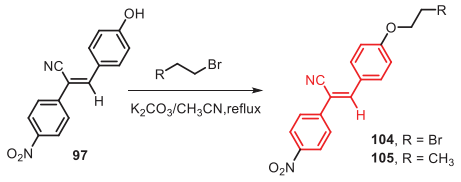

Scheme 12. Synthesis of compounds **104** and **105**.

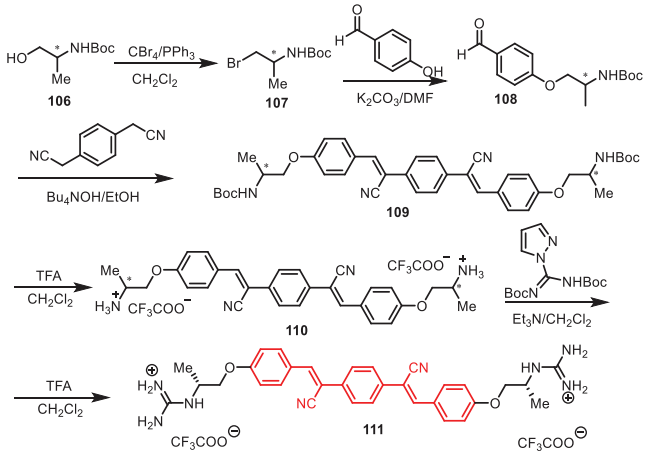

Scheme 13. Synthesis of compound **111**.

As a simple AIE compound, **104** was synthesized by Zheng's group as depicted in Scheme 12 [42]. After adding **104** into the mixture of (1*S*,2*R*)-**88** and enantiomers of chiral acids could obtain gel, suspension or precipitates, which showed a different intensity of fluorescence. As shown in Fig. S5A (Supporting information), **104** in suspension from mixing (1*S*,2*R*)-**88** and (*R*)-**11** emitted strong fluorescence, while **104** in transparent gel of (1*S*,2*R*)-**88** and (*S*)-**11** showed weak emission. For acid **99**, **100**, **20** and **9**, similar phenomena were observed (Table S2 in Supporting information). For acid **101** and **81**, one enantiomer caused precipitates while the other gave transparent gel with different fluorescence intensity, and the enantioselectivity was 6.6 and 46, separately. In the case of **74** and **21**, one enantiomer formed opaque gel while another resulted in suspension or precipitates. In addition, the content of one enantiomer is linearly related to fluorescence intensity (Fig. S5B in Supporting information), so the enantiomer purity of chiral acid could be determined easily.

In 2017, the group of Shinkai reported that AIE compound **111** containing two chiral spacers could discriminate two enantiomers of 1,2-cyclohexanedicarboxylic acid **66** [43]. As shown in Scheme 13, compound **111** was synthesized in several steps by commercial material **106**. In a mixed solvent of water and methanol, **111** was almost nonfluorescent. After adding **66**, the fluorescence intensity of mixture was obviously increased, and *RR*-**66** caused 10 times higher emission than *SS*-**66** (Figs. 5A and B). Fluorescence microscopic images of the self-assembly morphologies indicated that compound **111** associated with sterically favorable *RR*-**66**, and delivered the fibrous supramolecular aggregate (Fig. 5C), whereas **111** combined with sterically less favorable *SS*-**66**, and afforded the finite aggregate (Fig. 5D).

Base on the structure of cyanostilbene, *R*-**113** and *S*-**113** were facilely synthesized by our group (Scheme 14) [44]. To our delight, *R/S*-**113** could selectively discriminate the enantiomers of chiral acidic compounds and amino acids with good enantioselectivity through acid-base and H-bonding interactions. As shown in Figs. S6A and B (Supporting information), the suspensions formed from a mixture of D-**100** or D-**26** and *R*-**113**, but the mixture of L-**100** or

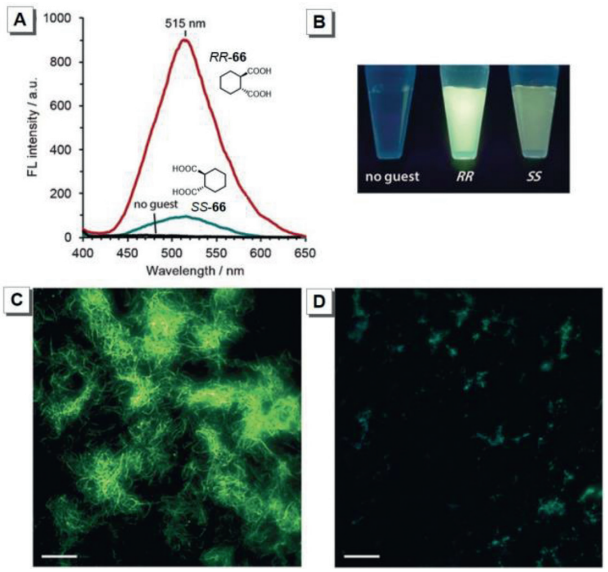

Fig. 5. (A) Fluorescence spectra of **111** in the presence of *RR*-and *SS*-**66** (1.0 mm for both) and (B) the corresponding photograph. Fluorescence microscopic images of the dispersions of **111**/*RR*-**66** (C) and **111**/*SS*-**66** (D). Conditions: [**111**] = 50 μmol/L, [**66**] = 1.0 mmol/L. Scale bar: 10 μm. Reprinted with permission [43]. Copyright 2017, Wiley-VCH Verlag GmbH & Co. KGaA.

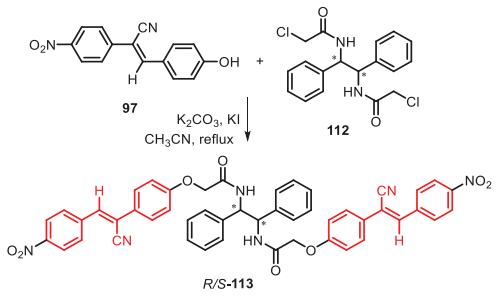

Scheme 14. Synthesis of chiral AIEgens *R/S*-**113**.

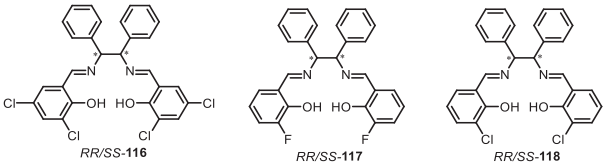

Scheme 15. Chemical structures of **116**, **117** and **118**.

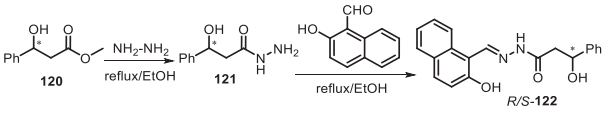

Scheme 16. Synthesis of compounds *R/S*-**122**.

L-**26** with *R*-**113** still maintained in solution. Enantioselectivity of two enantiomers of **100** and **26** were 17.9 and 5.9, respectively. For other chiral carboxylic acids depicted in Table 10, *R*-**113** could differentiate their enantiomers with the fluorescence intensity ratio from 2.06 to 4.88. Due to the linear relationship between the fluorescence intensity and enantiomer composition, an unknown enantiomer excess value of **100** could be determined (Fig. 6C). Interestingly, *R*-**113** also could detect arginine from 23 kinds of racemic amino acids or acidic compounds with a color change (Figs. S6D and E in Supporting information).

Table 10
Fluorescence intensity ratio and the mixture of enantiomers of analytes with *R*-**113** in various solvent(s).

No	Analytes	I_1/I_2	Mixtures[a]
1	**100**	17.9 (D/L)	1×10^{-5} M in DMF: $H_2O = 3/2$
2	**74**	3.89 (D/L)	1×10^{-4} M in DMF:$H_2O = 3/2$
3	**12**	3.66 (*S*/*R*)	0.67×10^{-4} M in DMF: $H_2O = 2/3$
4	**6**	3.49 (L/D)	1×10^{-4} M in DMF: $H_2O = 3/2$
5	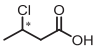 **114**	3.38 (L/D)	1×10^{-4} M in DMF
6	**54**	2.36 (L/D)	1×10^{-4} M in DMSO: $H_2O = 3/2$
7	**7**	2.19 (L/D)	1×10^{-4} M in DMSO: $H_2O = 3/2$
8	**5**	2.15 (D/L)	1×10^{-4} M in DMF: $H_2O = 3/2$
9	**11**	2.07 (*R*/*S*)	1×10^{-4} M in DMF: $H_2O = 3/2$
10	**26**	5.9 (D/L)	1×10^{-5} M in DMF: $H_2O = 2/3$
11	**53**	4.88 (L/D)	1×10^{-5} M in DMF: $H_2O = 3/2$
12	**22**	4.21 (L/D)	1×10^{-5} M in DMF: $H_2O = 3/2$
13	**23**	3.40 (L/D)	0.84×10^{-4} M in DMF: $H_2O = 1/1$
14	**24**	2.51 (L/D)	0.84×10^{-4} M in DMF: $H_2O = 1/1$
15	**73**	2.16 (D/L)	1×10^{-4} M in DMSO
16	**83**	2.11 (L/D)	1×10^{-4} M in DMF
17	**27**	2.06 (L/D)	1×10^{-4} M in DMF
18	 **115**	4.86 (D/L)	1×10^{-5} M in DMSO: $H_2O = 3/2$

[a] M = mol/L.

Table 11
Photophysical data of (*R*,*R*)-**116** and (*S*,*S*)-**116** DMSO solution upon the addition of 100 equiv. of different D- or L-amino acids.

No	Analytes	(*R*,*R*)-**116**		(*S*,*S*)-**116**	
		I/I_0	$(I_D\text{-}I_0)/(I_L\text{-}I_0)$	I/I_0	$(I_D\text{-}I_0)/(I_L\text{-}I_0)$
1	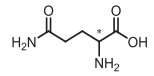 **119**	6.89 (L)	2.93	5.82 (L)	6.22
		20.2 (D)		36.2 (D)	
2	**27**	20.3 (L)	0.91	15.8 (L)	2.827
		18.5 (D)		35.8 (D)	
3	**29**	6.46 (L)	0.84	2.95 (L)	2.13
		5.43 (D)		6.31 (D)	
4	**28**	4.67 (L)	2.46	4.46 (L)	2.71
		11.5 (D)		12.3 (D)	

4. Chiral recognition by Schiff base derivatives

Schiff base derivatives occupy an importance position in analysis and detection of compounds [45]. For instance, Schiff bases **116**-**118** (Scheme 15) could be used as chiral probes of unprotected amino acids with different fluorescence intensity [46]. As shown in Table 11, Tables S3 and S4 (Supporting information), adding different amino acids to Schiff base solutions would enhance their fluorescence. *R*,*R*-**116** could discriminate the enantiomers of **119** and **28** with $(I_D\text{-}I_0)/(I_L\text{-}I_0)$ of 2.93 and 2.46, respectively. *S*,*S*-**112** could discriminate the enantiomers of **119**, **27**, **29** and **28** with $(I_D\text{-}I_0)/(I_L\text{-}I_0)$ of 6.22, 2.827, 2.13 and 2.71, respectively. *R*,*R*-**117** had an excellent $(I_D\text{-}I_0)/(I_L\text{-}I_0)$ of 4.89 for enantioselective recognition of D- and L-**27**. *S*,*S*-**117** could discriminate enantiomers of **28** ($(I_D\text{-}I_0)/(I_L\text{-}I_0) = 0.11$). In addition, *R*,*R*-**118** or *S*,*S*-**118** also showed high $(I_D\text{-}I_0)/(I_L\text{-}I_0)$ value for enantiomers of **27**, **119** and **29**.

Schiff bases *R*-**122** could be prepared by nucleophilic reactions of amine **121** and 2-hydroxy-1-naphthaldehyde and could discriminate the enantiomers of **34** and **18** by the intermolecular hydrogen bonds (Scheme 16) [47]. The $(I_S\text{-}I_0)/(I_R\text{-}I_0)$ values of enantiomers of **34** and **18** were 0.4 and 0.36, respectively.

Chiral *R*,*R*-**125** and *S*,*S*-**126** were synthesized in short steps (Scheme 17) [48]. Because of the nonconjugated, flexible and multidentate structure of probes, they might form cavity easily for discriminating enantiomers of **42**, and the $(I_S\text{-}I_0)/(I_R\text{-}I_0)$ value of *R*,*R*-**125** and *S*,*S*-**126** are 0.38 and 3.59 for enantioselective recognition of *R*/*S*-**42**, respectively.

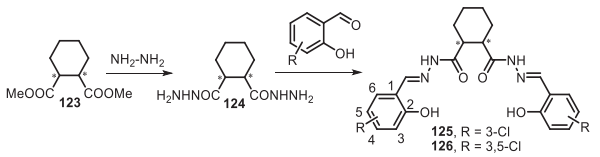

Scheme 17. Synthesis of **125** and **126**.

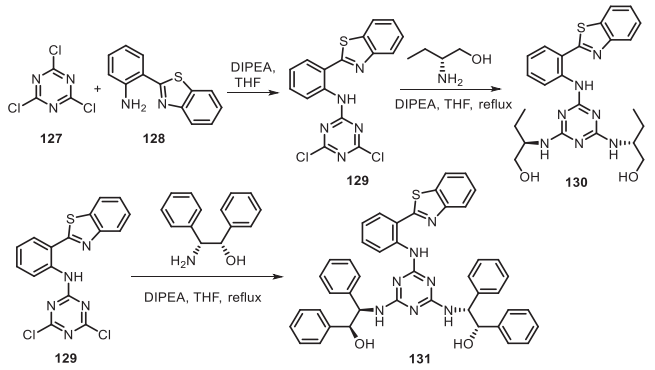

Scheme 18. Synthesis of compounds **130** and **131**.

Table 12
Fluorescence intensity and intensity ratio of the mixture of *R*/*S*-carboxylic acids with **130** and **131** in DMSO:H_2O = 40:60.

No	Analytes	**130**		**131**	
		I	I_R/I_S	*I*	I_R/I_S
1	 **132**	200.9 (*R*)	1.69	245.1 (*R*)	1.44
		119.0 (*S*)		169.8 (*S*)	
2	**12**	326.4 (*R*)	2.59	777.2 (*R*)	2.42
		126.1 (*S*)		320.9 (*S*)	
3	**11**	426.5 (*R*)	2.06	713.0 (*R*)	2.2
		207.0 (*S*)		324.4 (*S*)	
4	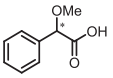 **133**	202.1 (*R*)	1.35	628.1 (*R*)	1.38
		149.2 (*S*)		455.6 (*S*)	

5. Chiral recognition by other AIE derivatives

Apart from the AIE derivatives mentioned above, other AIE derivatives, such as compounds **130** and **131** also could be used for chiral recognition [49]. As shown in Scheme 18, **130** and **131** were synthesized by Bozkurt's group in two steps. Thanks to the multiple hydrogen bonds and steric hindrance, 4 kinds of chiral carboxylic acids could be recognized with good enantioselectivity. As depicted in Table 12, all enantiomers could enhance the fluorescence intensity of AIE compounds, and the *R*-enantiomer lead stronger emission than *S*-enantiomer. Compound **130** could discriminate enantiomers of **132**, **12**, **11** and **133** with enantioselectivity of 1.69, 2.59, 2.06 and 1.35, respectively. Similarly, the fluorescence intensity ratio between **131** and enantiomers of **132**, **12**, **11** and **133** were also obtained with 1.44, 2.42, 2.2 and 1.38.

6. Conclusions and outlook

The study of chiral AIEgens in enantioselective recognition were summarized in this review. Four kinds of AIEgens including TPE derivatives, α-cyanostilbene derivatives, Schiff base derivatives and

other AIE derivatives were discussed from their synthesis, recognition capabilities and proper mechanisms. Chiral AIE-active probes are generally designed in structure to include three key factors: a chromophore, binding site and chiral source. Compared with traditional chiral organic probe, chiral AIEgens can detect acids, amino acids, amines and alcohols with excellent enantioselectivity and high emission efficiency in the aggregated state. The sensing mechanism for AIEgens primarily contain acid-base interaction, hydrogen bonding, CH-π interaction and host-guest interaction. In addition, the AIE-active macrocycle could also enhance the enantioselectivity for chiral analytes through encapsulation of guest molecules with suitable size. These conclusions can give some significant guidance for chiral molecular design and synthesis and entice more readers to contribute their efforts to chiral AIE research.

But as a whole, the study of AIEgens for chiral recognition is still in infancy and much more work is needed to be done to enrich this area. Up to now, the analytes are mainly focused on simple acids, amines or alcohols, design and synthesis of novel chiral AIEgens with general applicability will have an increased demand. The most reported chiral AIEgens discriminate two enantiomers mainly through monitoring the change of fluorescence intensity, some novel probes showing intuitional color change upon complexation with chiral analytes are required and the further applications of chiral AIEgens need to be expanded.

Declaration of competing interest

The authors declare that they have no known competing financial interests or personal relationships that could have appeared to influence the work reported in this paper.

Acknowledgments

This work was partially supported by the National Natural Science Foundation of China (Nos. 52173152, 21805002), Guangdong Basic and Applied Basic Research Foundation (No. 2020A1515110476), the Fund of the Rising Stars of Shaanxi Province (No. 2021KJXX-48), Scientific and Technological Innovation Team of Shaanxi Province (No. 2022TD-36), and Scientific Research Program Funded by Shaanxi Provincial Education Department (No. 22JK0247).

Supplementary materials

Supplementary material associated with this article can be found, in the online version, at doi:10.1016/j.cclet.2022.108041.

Reference

[1] M.J. Genzink, J.B. Kidd, W.B. Swords, T.P. Yoon, Chem. Rev. 122 (2022) 1654–1716.
[2] D. Saha, A. Kharbanda, W. Yan, et al., J. Med. Chem. 63 (2020) 441–469.
[3] F. Corbo, C. Franchini, G. Lentini, et al., J. Med. Chem. 50 (2007) 1907–1915.
[4] J. Yu, Z. Yu, R.J. Capon, H. Zhang, Molecules 27 (2022) 1279.
[5] R.R. Miller, A. Feingold, J. Paxinos, JAMA 213 (1970) 996–1006.
[6] T. Ito, H. Handa, Congenit. Anom. 52 (2012) 1–7.
[7] R. Franzini, M. Pierini, A. Mazzanti, et al., Int. J. Mol. Sci. 22 (2021) 144.
[8] Z. Szakács, Z. Sánta, A. Lomoschitz, C. Szántay, Trend S, Anal. Chem. 109 (2018) 180–197.
[9] G. Neumajer, T. Sohajda, A. Darcsi, et al., J. Pharm. Biomed. 62 (2012) 42–47.
[10] Y. Zhao, Y. Wang, X. Zhang, ACS Appl. Mater. Interfaces 9 (2017) 20991–20999.
[11] L. Pu, Chem. Rev. 104 (2004) 1687–1716.
[12] L. Pu, Acc. Chem. Res. 45 (2012) 150–163.
[13] X. Zhang, J. Yin, J. Yoon, Chem. Rev. 114 (2014) 4918–4959.
[14] J. Weiss, Nature 152 (1943) 176–178.
[15] W. Li, J. Wang, Y. Xie, et al., Prog. Org. Coat. 120 (2018) 1–9.
[16] X. Tang, H. Jiang, Y. Si, et al., Chem 7 (2021) 2771-2786.
[17] B. Zhao, K. Pan, J. Deng, Macromolecules 51 (2018) 7104–7111.
[18] J. Luo, Z. Xie, J.W.Y. Lam, et al., Chem. Commun. (2001) 1740–1741.
[19] Y. Chen, J.W.Y. Lam, R.T.K. Kwok, et al., Mater. Horiz. 6 (2019) 428–433.
[20] H. Feng, J.W.Y. Lam, B.Z. Tang, Coord. Chem. Rev. 406 (2020) 213142.
[21] M. Kang, Z. Zhang, N. Song, et al., Aggregate 1 (2020) 80–106.
[22] J. Zhang, B. He, Y. Hu, et al., Adv. Mater. 33 (2021) 2008071.
[23] W. Lu, S. Wei, H. Shi, et al., Aggregate 2 (2021) e37.
[24] H. Bai, W. He, J.H.C. Chau, et al., Biomaterials 268 (2021) 120598.
[25] H. Li, H. Kim, J. Han, et al., Aggregate 2 (2021) e51.
[26] M. Hu, H. Feng, Y. Yuan, et al., Coord. Chem. Rev. 416 (2020) 213329.
[27] H. Feng, Y. Yuan, J. Xiong, Y. Zheng, B.Z. Tang, Chem. Soc. Rev. 47 (2018) 7452–7476.
[28] N. Liu, S. Song, D. Li, Y. Zheng, Chem. Commun. 48 (2012) 4908–4910.
[29] L. Pu, Angew. Chem. Int. Ed. 59 (2020) 21814–21828.
[30] H. Feng, X. Zhang, Y. Zheng, J. Org. Chem. 80 (2015) 8096–8101.
[31] J. Xiong, W. Xie, J. Sun, et al., J. Org. Chem. 81 (2016) 3720–3726.
[32] M. Kawai, A. Hoshi, R. Nishiyabu, Y. Kubo, Chem. Commun. 53 (2017) 10144–10147.
[33] X. Zhang, Q. Yu, W. Lu, S. Chen, Z. Dai, Tetrahedron Lett. 58 (2017) 3924–3927.
[34] M. Hu, Y. Yuan, W. Wang, et al., Nat. Commun. 11 (2020) 161.
[35] S. Xiang, P. Lv, C. Guo, et al., Chem. Commun. 57 (2021) 13321–13324.
[36] X. Wang, S. Xiang, C. Qi, et al., ACS Nano 16 (2022) 8223–8232.
[37] P. Mahalingavelar, S. Kanvah, Phys. Chem. Chem. Phys. 24 (2022) 23049–23075.
[38] Y. Zheng, Y. Hu, J. Org. Chem. 74 (2009) 5660–5663.
[39] D. Li, Y. Zheng, J. Org. Chem. 76 (2011) 1100–1108.
[40] Y. Zheng, Y. Hu, D. Li, Y. Chen, Talanta 80 (2010) 1470–1474.
[41] D. Li, Y. Zheng, Chem. Commun. 47 (2011) 10139–10141.
[42] D. Li, H. Wang, Y. Zheng, Chem. Commun. 48 (2012) 3176–3178.
[43] T. Noguchi, B. Roy, D. Yoshihara, et al., Angew. Chem. Int. Ed. 56 (2017) 12518–12522.
[44] M. Chen, C. Qi, Y. Yin, et al., Org. Chem. Front. 9 (2022) 5160–5167.
[45] J. Wang, Q. Meng, Y. Yang, et al., ACS Sens. 7 (2022) 2521–2536.
[46] G. Shen, F. Gou, J. Cheng, et al., RSC Adv. 7 (2017) 40640–40649.
[47] M. Wang, C. Cheng, J. Song, et al., Chin. J. Chem. 36 (2018) 698–707.
[48] M. Wang, C. Cheng, C. Li, et al., J. Mater. Chem. C 7 (2019) 6767–6778.
[49] E. Halay, S. Bozkurt, Chirality 30 (2018) 275–283.